EUROPEAN ORGANIZATION FOR NUCLEAR RESEARCH

EUROPEAN LABORATORY FOR PARTICLE PHYSICS (CERN)

LEP Energy Group/96-01
ALEPH 96-106
PHYSIC 96-097
July 1996

Preliminary Centre-of-Mass Energy Corrections from Dispersion and Collision Offsets for the 1995 Scan

P. Puzo [1)], **J. Yamartino** [2)]

1) CERN, SL Division, Geneva   2) University of Wisconsin, Madison

Abstract

The Vernier scan and collision offset analysis for the 1995 energy scan is presented. The procedure to fit the Vernier scan data to obtain the optimal Vernier setting is described. Roughly 35 Vernier scans were performed at each IP and at each off peak energy point for the purposes of controlling collision offsets. The stability of the optimal Vernier setting (at each energy and IP) is found to be 0.8 - 1.8 μm and collision offsets are measured to be $\leq$ 0.5 μm (with a precision of $\sim$ 0.2 to 0.3 μm) over the course of the 1995 energy scan. Dispersion difference measurements were performed at each IP and at each energy point and found to be $\sim \pm 2 \ \ mm$ at each IP. Combining the results for the collision offsets and dispersion measurements leads to a determination of the centre-of-mass energy shifts. The uncertainty of the energy shifts are determined to be 0.3 to 0.6 MeV at each off peak point. This includes systematic errors which are discussed.

Contents

1 Introduction

The 1995 energy scan required the control of a new effect associated with the bunch-train bumps. These bumps generate opposite sign vertical dispersion at the interaction points of LEP. If the beams collide with a collision offset then the centre-of-mass energy is shifted from the nominal by an amount ΔE_{cm} [1]:

$$E_{cm} = E(e^+) + E(e^-) + \Delta E_{cm} \tag{1}$$

$$\Delta E_{cm} = -\frac{1}{2} \cdot \frac{\delta y}{\sigma_y^2} \cdot \frac{\sigma_E^2}{E} \cdot \Delta D_y^* \tag{2}$$

where δy, the collision offset, is the distance between the centre of the positron bunch and the electron bunch in collision at the IP, σ_y the individual beam size, ΔD_y^* the difference in the vertical dispersion ($D_{e^+}^* - D_{e^-}^*$) and E, σ_E are the beam energy and spread respectively.

As ΔD_y^* is a characteristic of the bunch train bumps and σ_E can not be reduced to zero the only practical control of this effect is to reduce δy as much as possible. In the 1995 energy scan, LEP was operated with 4 trains of 3 bunches per beam (4*3 + 4*3). Under such circumstances it not possible to collide all bunches with zero δy since the residual beam-beam kicks generate transverse distortions of the train [2]. It is shown in [1] that optimization of the total luminosity results in a cancellation of the individual ΔE_{cm} of each collision in the train provided that the dispersion differences are the same for each family (the three collisions in a train will be referred to as families a, b and c).

The strategy for controlling collision offsets [3] was to perform Vernier scans during each off-peak fill (once near the beginning of the fill and once near the end). A Vernier scan is an automatic procedure which uses the vertical separators to scan the colliding beams across each other. The LEP luminosity monitors measure the luminosity of each family at each separation step in the Vernier scan. The luminosity as a function of the separation indicates the Vernier setting for maximum luminosity for each family. The average of the three families gives the *optimal* Vernier setting.

Additionally, the opposite sign vertical dispersion must also be measured in order to set the size of the effect. This was also done with Vernier scans. This technique will be described in section 3.

2 Vernier Scans

This section will describe the procedure for performing Vernier scans and the status of the Vernier scan fit, stability, beam size and collision offset analyses.

2.1 Online Procedures

During the 1995 energy scan, the Vernier scans were preformed in the following way:

- Typically, there were 8 steps in the scan each separated by 2 μm. The number of steps and the step size could be changed for special circumstances.
- Three consecutive luminosity measurements (with errors) were recorded for each family for each Vernier setting. The length of each measurement was 9 seconds. The

redundancy allowed a test of the errors which is important for understanding the fits to the data.
– Vernier scans were done only at one IP at a time.
– The Vernier scan data were stored in the LEP measurement database for offline analysis.

Vernier scans typically took about 8 minutes to conduct. An online program would fit the data for the three families to a gaussian and return the optimal position for each family as well as the average optimal position. The operators would use this average optimal position to adjust the Vernier setting thus controlling the collision offsets. If there was a problem with the scan the operator could choose to perform the scan again. The Vernier settings (either during a Vernier scan or not) were logged for offline analysis. Figure 1 shows the display of a series of Vernier scans as it appeared in the LEP control room.

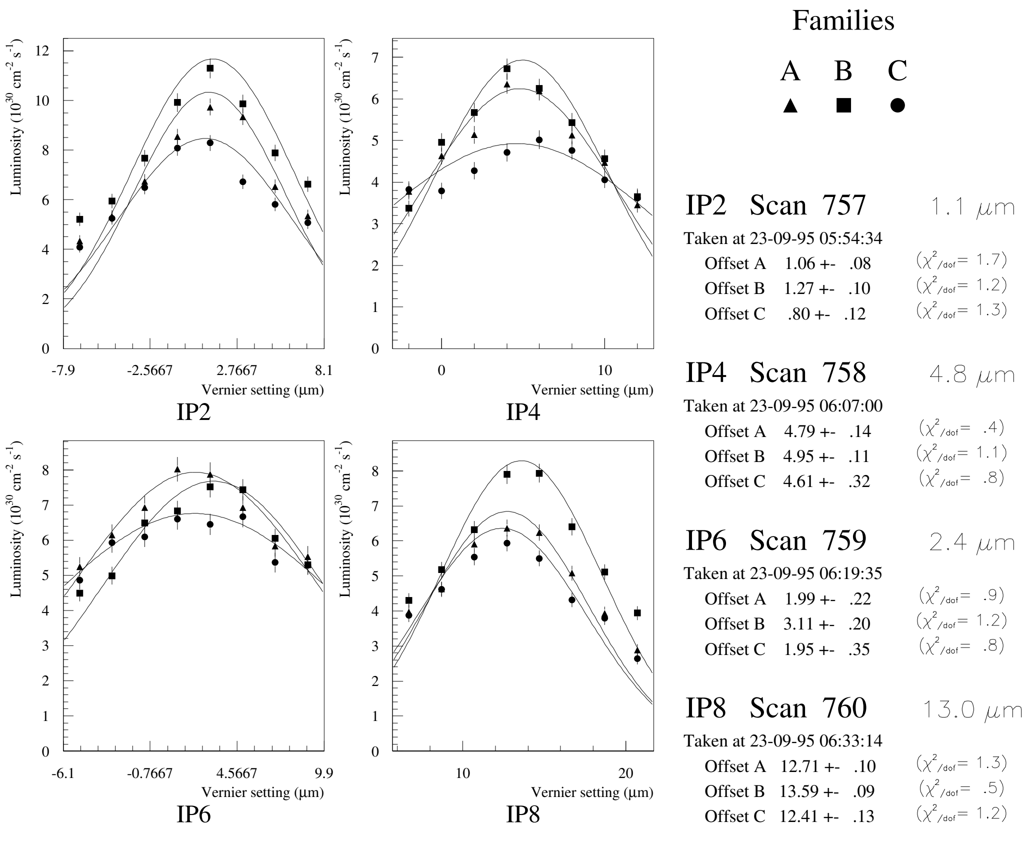

Figure 1: *Typical online display of Vernier scans taken at each IP. On the left , the four plots display the last Vernier scan in each of the four IP's. Curves are gaussian fits to the data. On the right , the offsets per family are shown together with their weighted mean. The operators adjust the Vernier setting to this mean.*

2.2 Fit Analysis

The Vernier scan data were re-analyzed offline to study quality, stability and other characteristics of the scans. To start, the data were fit as they were online. It was noticed early in the energy scan that the χ^2 of the fits were too high. An analysis of the 3 consecutive measurements of the luminosity [4] indicated that there were fluctuations in the measurements beyond the reported error, thus the high χ^2. This was traced to an integer truncation of the data when it was transferred from the IP to the control room. After the problem was corrected (after Vernier scan number 587) the data appear to fluctuate in accordance with the reported error [5] and the χ^2 reduced by a factor of two. Figure 2 shows the difference between two consecutive luminosity measurements divided by the combined error. This should be a gaussian with an rms of 1. The left plot shows the distribution for data taken before the fix with an rms of 1.4 and the right plot shows the same after the fix. The rms in that case is 1.03. Note the quality of this gaussian fit to $\pm 4\sigma$ indicating that the luminosity measurements and errors are quite reliable.

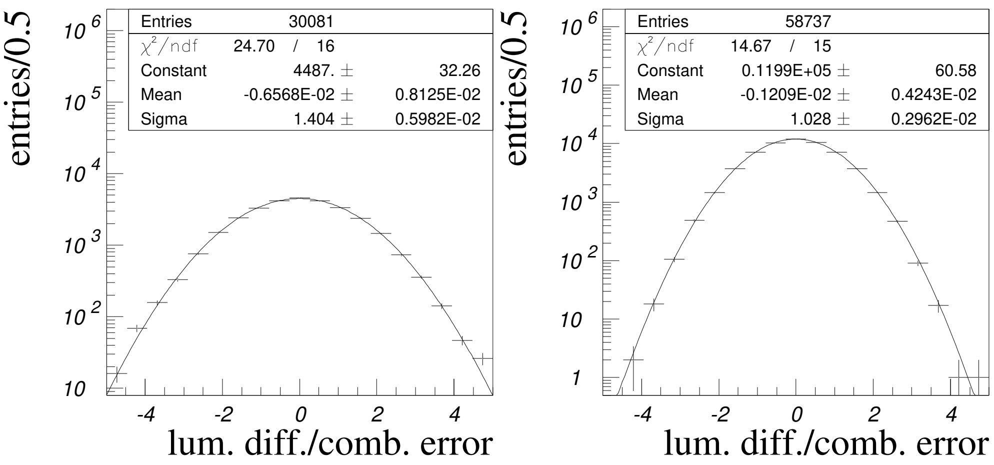

Figure 2: *The difference between consecutive luminosity monitor measurements divided by their combined error. Left: For those data taken with the data truncation problem (Sigma = 1.40). Right: For those data taken after the problem was fixed (Sigma = 1.03).*

Vernier scans 380 to 974 comprise those Vernier scans taken during the 1995 energy scan. For each off peak energy and each IP there were $\sim$ 35 "good" [1] Vernier scans performed for the purposes of controlling collision offsets for a total of 280 Vernier scans.

The χ^2 per degree of freedom of each fit is shown in figure 3. The number of degrees of freedom is typically 21 and there are 3 fits per Vernier scan for a total of (3×280) 840 fits. The data taken prior to the data truncation problem have their errors inflated by an amount indicated by their fluctuations (factor 1.4). One can see that when this problem is corrected the fit to a gaussian is quite good. The typical statistical error on the optimal Vernier position per family is 0.2 - 0.3 μm. The χ^2 is observed to average slightly higher than 1 indicating that a gaussian fit is not the exact description of the luminosity vs. separation relation. One possible explanation would be the changing beam size which is sometimes associated with Vernier scans. This effect will be addressed in the section 2.4.

[1] "good" here refers to those Vernier scans where the logged data are complete, the Vernier scan did not have other problems (usually given in the logbook), and were not taken for other purposes.

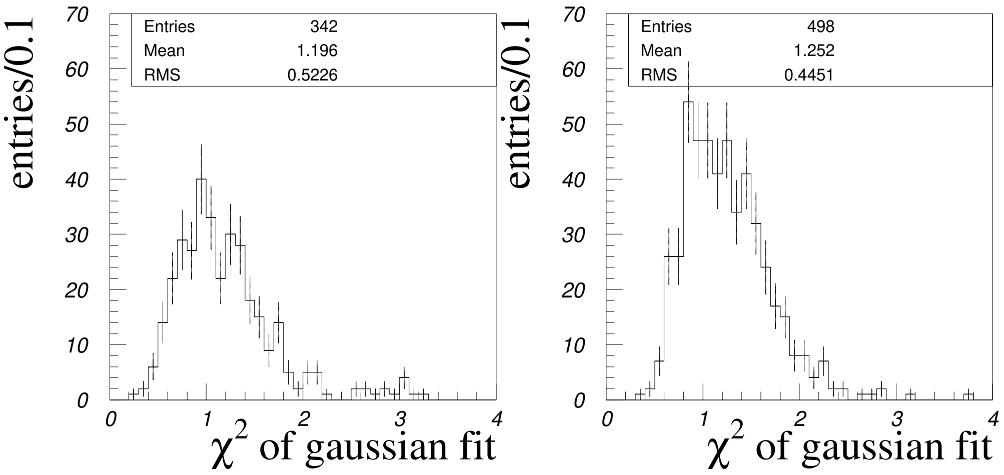

Figure 3: *The χ^2 per degree of freedom distribution for gaussian fits of the Vernier scans used in the analysis of collision offsets. Left: The χ^2 distribution for Vernier scans taken prior to correction of data truncation problem (errors inflated). Right: The distribution for those taken after the problem was fixed.*

2.3 Stability

The stability of the optimal position is shown in figure 4 for IP2 as a function of time into the 1995 energy scan running period (time since Aug. 1, 1995). The mean and rms variation of the optimal position for each IP is given in table 1. It is noted that the mean optimal position at each IP is different for each energy. This fact was noticed early in the energy scan and resulted in different sets of initial Vernier settings for the two off peak points. The error on the mean is simply the rms divided by $\sqrt{N_s}$, where N_s is the number of Vernier scans taken at the IP and energy.

2.4 Vertical Beam Size

It is known that the vertical size of the beams may change during a Vernier scan. This was first observed with the BEUV [6]. It is therefore necessary to correct for this variation when making the fit to the luminosity data. The BEUV records the mean spot size of the families in a train and therefore cannot be used to correct an individual family as the variation may be different for each family.

Since the variation of the beam size results in variations of the luminosity, it is possible to use the luminosity of the other IP's during the scan to estimate the changing beam size [10]. It is found that the correction to the optimal Vernier setting (for all IP's and families) is less than 0.1 μm indicating no bias from this effect. The rms is 0.4 μm and is small compared to the rms stability shown in table 1. It is therefore expected to have little effect on it. The correction reduced the mean χ^2 of the fits from $\sim$ 1.2 to $\sim$ 1.1. The breakdown of this correction is given in table 2.

Another important quantity to come out of the Vernier scan fits is the vertical beam size itself (σ_y) since the centre-of-mass energy effect is (according to eq. 2) inversely proportional to the square of the beam size.

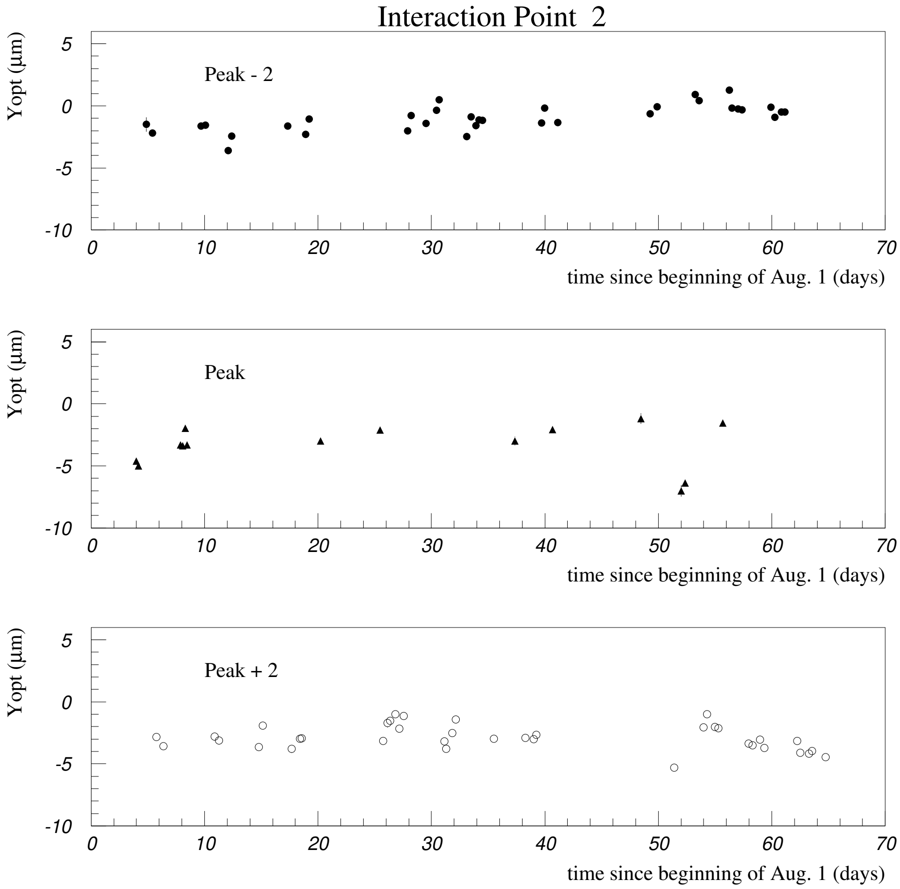

Figure 4: *The stability of the optimal Vernier setting for IP2 during the 1995 energy scan.*

It is important to note that beam size is observed to decrease as the time into the fill increases [11]. This can be seen in Figure 5 which shows the beam size in μm as a function of the number of hours into the fill. The data have been fit to a straight line. Note that the error on the beam size coming from the fit is $\approx$ 0.2 μm. We have artificially increased this error to 0.5 μm to improve the quality of the linear fit. This 0.5 μm will be taken as a systematic error on the beam size.

Typically the slope of the beam size decrease is $\approx$ 0.10 to 0.15 μm per hour. The fit at each off peak energy and each IP is used as a simple model of the beam size as a function of time into the fill. Since the correction is proportional to the inverse square of the beam size, we determine the luminosity weighted average of this such that the appropriate mean beam size, $\overline{\sigma}_y$, is used to determine the scale of the energy shifts. We therefore have:

$$\overline{\sigma}_y = \frac{1}{\sqrt{\langle \frac{1}{\sigma_y^2} \rangle_{lum}}} \tag{3}$$

Table 3 shows the average vertical beam size, $\overline{\sigma}_y$, for each IP and energy. One observes that there are significant differences in the vertical beam sizes at different IP's. This, in principle, could be due to the overall Vernier scale (from high Voltage to μm) at each

Table 1: *The mean and rms variation of the optimal Vernier position (using a gaussian fit) for each IP during the 1995 energy scan. L3,ALEPH,OPAL and DELPHI are IP2,4,6 and 8 respectively.* N_s *is the number of Vernier scans.*

Optimal Vernier position			
IP	N_s	mean (μm)	rms (μm)
L3 Peak−2	34	-0.88 ± 0.19	1.07 ± 0.13
L3 Peak	14	-3.21 ± 0.44	1.57 ± 0.20
L3 Peak+2	37	-2.94 ± 0.16	0.97 ± 0.11
ALEPH Peak−2	34	6.25 ± 0.15	0.86 ± 0.11
ALEPH Peak	13	9.16 ± 0.33	1.15 ± 0.23
ALEPH Peak+2	37	9.57 ± 0.19	1.11 ± 0.13
OPAL Peak−2	34	-0.88 ± 0.25	1.41 ± 0.18
OPAL Peak	13	-3.12 ± 0.36	1.24 ± 0.25
OPAL Peak+2	37	-3.23 ± 0.25	1.50 ± 0.18
DELPHI Peak−2	34	14.12 ± 0.17	0.98 ± 0.12
DELPHI Peak	13	15.33 ± 0.39	1.35 ± 0.28
DELPHI Peak+2	38	15.71 ± 0.20	1.24 ± 0.14

IP. It could also be due to real differences in beam sizes which could be correlated to luminosities. If there is an overall difference in the Vernier scale it can be seen that this scale difference drops out of equation 2 since the collision offset, δy, and the dispersion difference, ΔD_y^*, are also subject to the same scale differences.

Also noted is the smaller beam sizes measured at peak $+\ 2$ compared to peak $-\ 2$. This effect is due to the fact that the conversion from Volts on the separators to micron movement of the beam was a constant and used the nominal Z^o peak energy [7]. Since this conversion is proportional to the inverse of the beam energy, and the off peak energies are 2% different than the nominal, one can see that the beam sizes are actually similar at the off peak points. We use the average beam size (3.9, 5.3, 4.8, 4.1 μm at IP 2,4,6 and 8) at each IP. This 2% effect is ignored in all other aspects of this analysis.

Table 2: *The mean and rms of the correction to the optimal Vernier setting due to beam size variation during a vernier scan.*

Shift of optimal Vernier setting		
IP	mean (μm)	rms (μm)
L3 family a	-0.02 ± 0.02	0.17
b	0.10 ± 0.03	0.23
c	0.07 ± 0.08	0.63
ALEPH family a	-0.06 ± 0.02	0.17
b	0.06 ± 0.03	0.22
c	-0.14 ± 0.06	0.52
OPAL family a	-0.06 ± 0.03	0.30
b	-0.02 ± 0.05	0.45
c	-0.20 ± 0.07	0.66
DELPHI family a	-0.05 ± 0.02	0.16
b	0.12 ± 0.04	0.34
c	-0.06 ± 0.02	0.18

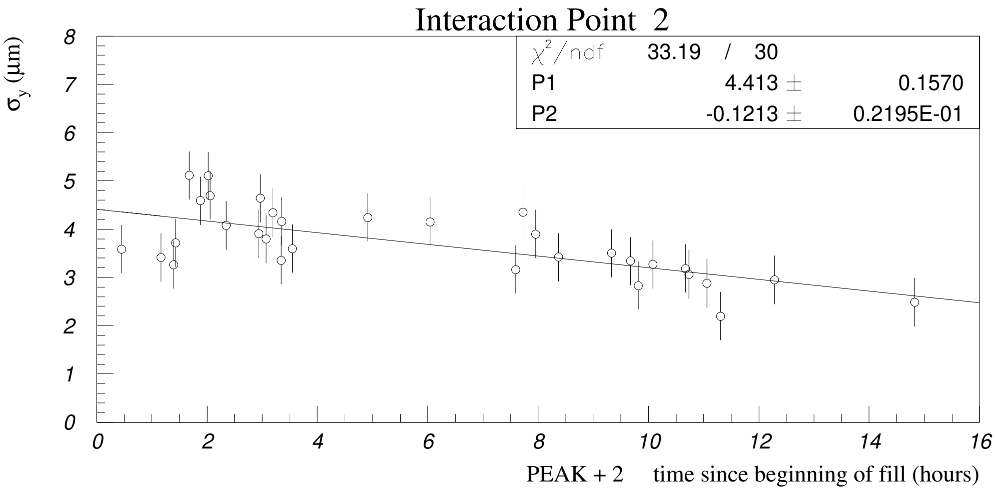

Figure 5: *The evolution of the vertical beam size as a function of time elapsed since the beginning of the fill.*

Table 3: *The mean vertical beam size* $\overline{\sigma}_y$

Vertical beam size in μm	
IP	$\overline{\sigma}_y$ (μm)
L3 Peak−2	4.00 ± 0.12
L3 Peak+2	3.78 ± 0.07
ALEPH Peak−2	5.41 ± 0.08
ALEPH Peak+2	5.18 ± 0.10
OPAL Peak−2	4.94 ± 0.11
OPAL Peak+2	4.58 ± 0.07
DELPHI Peak−2	4.24 ± 0.13
DELPHI Peak+2	3.94 ± 0.06

2.5 Collision Offsets

In order to calculate the collision offset it is necessary to compare the optimal Vernier setting, y_{opt}, with the *actual* Vernier setting, y_{set}. The collision offset, δy, is defined as:

$$\delta y = y_{set} - y_{opt} \tag{4}$$

We will determine δy each 15 minutes for the purposes of evaluating the centre-of-mass energy shifts given by eq. 2. Since y_{opt} is measured only once or twice during a fill we will need to model the true optimal position using these measurements. If a fill has 2 good Vernier scans then the y_{opt} is taken as the optimal position of the first scan up until the time of the first scan. In the time between both scans, y_{opt} is a linear interpolation between the two Vernier scan measurements and after the second Vernier scan, y_{opt} is taken as the optimal position of the second Vernier scan. In the case of a single Vernier scan in a fill, y_{opt} is the result of that one scan. In the case of no Vernier scan in a fill (which accounts for less than 10% of the integrated luminosity), the mean for the energy scan period at that IP and energy is taken as y_{opt}.

The Vernier setting is taken as the logged values. Only those settings which last for longer than 5 minutes are considered. At each 15 minute interval, the local y_{opt} and y_{set} are used to determine the collision offset δy. We give below in table 4 the mean collision offset at each IP and energy for the 1995 energy scan. The mean is weighted by the luminosity from IP4 for illustration and for the purposes of determining the errors. Each experiment will do its own weighting based on the data they use to measure the cross section.

The luminosity weighted collision offset, $\langle \delta y \rangle_{lum}$, is given by

$$\langle \delta y \rangle_{lum} = \langle y_{set} \rangle_{lum} - \langle y_{opt} \rangle_{lum} \tag{5}$$

Therefore, the error on $\langle \delta y \rangle_{lum}$ comes from the error on $\langle y_{opt} \rangle_{lum}$ since it is not known at all times and has a large RMS variation. The reproducibility error of the Vernier settings is already included in the RMS variation of the Vernier scan results. The statistical error of the collision offset is then taken as the RMS of the $\langle y_{opt} \rangle_{lum}$ distribution divided by $\sqrt{N_s}$ where N_s is the number of Vernier scans done at each IP and at each energy.

Note that the collision offset at peak $-$ 2 is, in each IP, larger than the collision offset at peak $+$ 2. This is due to the fact that the mean optimal position at peak $-$ 2 is systematically different from peak $+$ 2. Since this was fact was not anticipated, the Vernier settings were initially set between the the two optimal positions creating the observed behaviour of the mean collision offsets. The implications of this will be discussed in section 4.

3 Dispersion measurements

The dispersion difference ΔD_y^* is measured by observing the shift Δy_{opt} in the optimal Vernier setting, due to a shift (accomplished by changing the RF frequency) in the LEP beam energy [8]. The shift in the optimal Vernier setting when the beam energy is changed is directly proportional to ΔD_y^*. The difference in the dispersion of the two beams is then given by:

$$\Delta D_y^* = -\frac{\alpha_c \cdot f_{RF}}{\Delta f_{RF}} \cdot \Delta y_{opt} \tag{6}$$

Table 4: *The luminosity weighted collision offset in* μm.

Luminosity weighted collision offsets	
IP	mean (μm)
L3 Peak-2	0.43 $\pm$ 0.17
L3 Peak	0.24 $\pm$ 0.36
L3 Peak$+2$	-0.05 $\pm$ 0.17
ALEPH Peak-2	0.53 $\pm$ 0.19
ALEPH Peak	0.11 $\pm$ 0.33
ALEPH Peak$+2$	-0.36 $\pm$ 0.19
OPAL Peak-2	0.34 $\pm$ 0.24
OPAL Peak	0.17 $\pm$ 0.30
OPAL Peak$+2$	0.15 $\pm$ 0.30
DELPHI Peak-2	0.18 $\pm$ 0.16
DELPHI Peak	0.57 $\pm$ 0.32
DELPHI Peak$+2$	-0.16 $\pm$ 0.24

where Δy_{opt} is the observed shift in the optimal Vernier setting when the RF frequency, f_{RF}, is shifted by Δf_{RF}. The momentum compaction factor is denoted by α_c [9].

Dispersion measurements were made for each IP at each energy. Five measurements were done at L3 and DELPHI, six at ALEPH and seven at OPAL. These results are summarized in table 5. An example of a dispersion measurement at L3 in given in Fig. 6, where the offsets measured for each family are displayed for the three energies. The dispersion is proportional to the offset difference between both off energy measurements. The dispersion value retained is the average over the three families. The three vernier scans done at nominal frequency before and after each off frequency scan are used as a consistency check.

The errors are described in table 6. The fluctuations of the different measurements are much larger than their statistical error and are quite different from one IP to another. The variation of the measurements is not understood at the moment. We therefore take the RMS as one of the errors.

The beam size correction error is the difference between measuring the dispersion using a gaussian fit to the data and using a beam size corrected fit [10].

Following Eq. 6, there are three ways of computing the dispersion if we use three different frequencies. In the example of Fig. 6, the dispersion computed from -50 Hz to $+50$ hz is consistent with the one computed using only one off frequency scan and the three nominal frequency ones. However, this is not the case for all sets of measurements. For that reason, we introduced an additional error ("consistency check") which corresponds to the variation of the mean dispersion, rejecting the sets of measurements were the dispersion were not consistent between the three computed values.

The mean dispersion being computed with the average over the three families, we introduced another error which corresponds to the fluctuations of the dispersion computed per family.

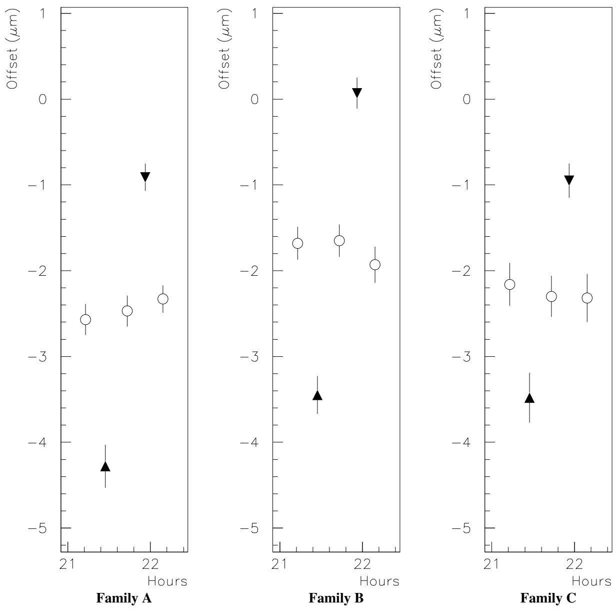

Figure 6: Example of a dispersion measurement at IP2 (L3 expt.) for the three families. The offsets for the three energies are displayed (○ for the nominal energy, ▲ and ▼ for Δf_{RF} = $+50$ and -50 Hz respectively).

Table 5: *Dispersion difference measurements at each IP.*

Dispersion difference ΔD_y^*	
IP	$\Delta D_y^*(mm)$
L3	2.0 ± 0.4
ALEPH	- 2.0 ± 0.7
OPAL	1.8 ± 0.8
DELPHI	- 1.5 ± 0.7

4 Energy shifts

Combining the results from the previous sections for mean collision offset, beam size and dispersion difference, we present the sensitivity (in $MeV/\mu m$) to collision offsets for each IP. The sensitivity, ϵ, is defined as follows (compare with eq. 2):

Table 6: ΔD_y^* *systematic errors associated with each IP.*

ΔD_y^* systematic errors (mm)				
	L3	ALEPH	OPAL	DELPHI
Fluctuations	0.2	0.7	0.6	0.5
Beam size correction	0.2	0.0	0.4	0.2
"Consistency check"	0.1	0.3	0.3	0.2
Family to family variations	0.2	0.2	0.0	0.5
Total error	0.4	0.7	0.8	0.7

$$\Delta E_{cm} = \epsilon \cdot \delta y \tag{7}$$

The sensitivity is presented in table 7 [2)].

We then combine this with the collision offsets given in table 4 to obtain an estimate of the centre-of-mass energy shifts at each IP and energy. This is shown in table 8. The error is due to the statistical error on the collision offset, δy, from table 4.

For Γ_Z, the important quantity is the difference between the corrections at the two off peak points. It is noted that this quantity is significant (on average) at each IP. This is due to the similar pattern of collision offsets seen in table 4. However, since the dispersion differences alternate in sign around the ring, the net effect is quite small. In fact, whereas each experiment will see an absolute correction to Γ_Z of $\sim$ 0.6 MeV (on average) the correction (from this effect alone) to the LEP average of Γ_Z will be $\sim$ 0.2 MeV. This is to be compared to the combined statistical and systematic error (see section 5.9).

Table 7: *Mean* ϵ *for each IP.*

Sensitivity $MeV/\mu m$	
IP	ϵ $(MeV/\mu m)$
L3	-2.3
ALEPH	1.3
OPAL	-1.4
DELPHI	1.6

5 Systematic studies

In this section we will present the results of systematic studies of the energy shifts.

2) We use the beam energy spread as determined from an analysis of the machine parameters and the z distribution of hadronic events in ALEPH [12].

Table 8: *The centre-of-mass energy correction ΔE_{cm}. The error is due to the error on the determination of the collision offset, δy.*

ΔE_{cm} for each Interaction Point	
IP	$\Delta E_{cm}(MeV)$
L3 peak-2	-0.99 $\pm$ 0.39
L3 peak	-0.55 $\pm$ 0.83
L3 peak+2	0.12 $\pm$ 0.39
ALEPH peak-2	0.69 $\pm$ 0.24
ALEPH peak	0.14 $\pm$ 0.41
ALEPH peak+2	-0.47 $\pm$ 0.24
OPAL peak-2	-0.48 $\pm$ 0.33
OPAL peak	-0.24 $\pm$ 0.41
OPAL peak+2	-0.21 $\pm$ 0.41
DELPHI peak-2	0.29 $\pm$ 0.25
DELPHI peak	0.91 $\pm$ 0.50
DELPHI peak+2	-0.26 $\pm$ 0.38

5.1 Reverse scans

One simple check of possible biases of the determination of the optimal Vernier setting from Vernier scans is to perform the scan in the opposite direction than it is normally preformed. The normal direction of scan was chosen for time considerations. The reverse direction of scan takes much longer due to the HV circuit (it's quicker to ramp the Voltage in one direction than in the other).

A reverse Vernier scan was done once at each IP immediately following a normal Vernier scan. The difference between the two is shown plotted in figure 7. The mean difference is $0.26 \pm 0.06\ \ \mu m$. A short term stability study [13] indicated that the rms variation of the optimal position is larger than the error on the mean at any given time. If these errors are used instead of the errors from the fit then the result is $0.25 \pm 0.16\ \ \mu m$. This makes the effect marginally significant. In either case the optimal position has been corrected by $0.13\ \ \mu m$ in order to allow for the possibility of bias and an error of $0.13\ \ \mu m$ is taken as a systematic error to cover the full difference.

5.2 Family shape

The difference between the optimal position for families a,b, and c gives a measurement of the shape of the trains. Figure 8 shows the difference between family a and b and family c and b for IP2 for peak - 2 fills throughout the energy scan. Table 9 shows the results for each IP.

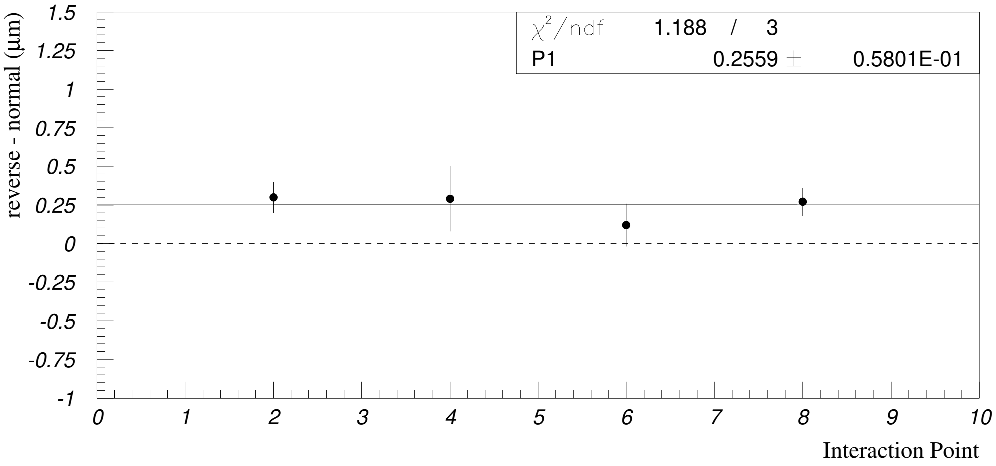

Figure 7: *Difference between reverse and normal Vernier scan.*

The rms variation of each measurement is $\sim 0.5\ \mu m$. Since the rms variation of the optimal Vernier setting is much larger than this the rms of the optimal setting is due to real drifts and not to fluctuations in the measurement of the optimal position. In other words, the families drift together.

The numbers in table 9 imply that the collision offset which is imposed on each family due to the overall luminosity optimization is $\sim 0.2 - 0.6\ \mu m$ (half of the numbers in table). This shape is a necessary input to further systematic studies of the effects of family to family variations indicated in the next section. In the limit of zero difference between the optimal position of the three families there is no error due to family to family variations of dispersion difference or relative luminosity response.

Table 9: *The mean family shape of the collision for each IP.*

Family Shape		
IP	$y_a - y_b(\mu m)$	$y_c - y_b(\mu m)$
L3 Peak-2	0.63 ± 0.09	0.63 ± 0.10
L3 Peak+2	0.80 ± 0.08	0.72 ± 0.09
ALEPH Peak-2	-0.56 ± 0.15	-0.73 ± 0.15
ALEPH Peak+2	-0.69 ± 0.08	-0.86 ± 0.13
OPAL Peak-2	0.57 ± 0.08	0.42 ± 0.12
OPAL Peak+2	0.40 ± 0.09	0.52 ± 0.09
DELPHI Peak-2	-1.30 ± 0.08	-1.01 ± 0.10
DELPHI Peak+2	-0.98 ± 0.07	-1.07 ± 0.08

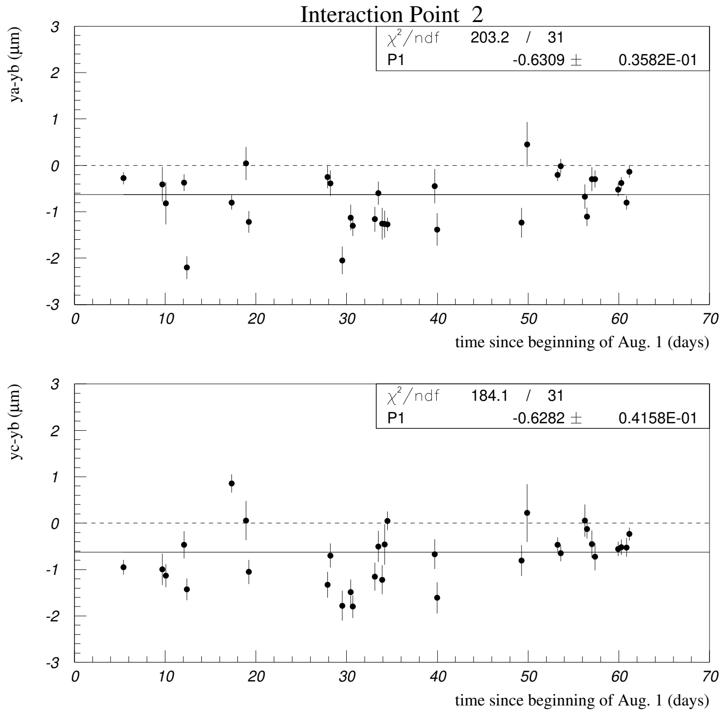

Figure 8: *The difference between the optimal Vernier position for the different families. Top plot: Family a compared to family b. Bottom plot: Family c compared to family b.*

5.3 Family to family variations

Family to family variations of the dispersion difference and/or luminosity monitor response can (in the presence of a train shape) lead to shift in the centre-of-mass energy even if the beams are colliding at the optimal position [1]. By using the measured train shape it is possible to determine the effect of family to family dispersion differences and/or luminosity monitor response differences. If we assume a family to family dispersion difference variation of 0.5 mm (the largest of this error from table 6) and a luminosity response variation of 10% we determine the following ΔE_{cm} errors at each IP shown in table 10.

Table 10: *The error on ΔE_{cm} due to dispersion difference and luminosity response variations.*

Error on ΔE_{cm} (MeV)			
IP	Dispersion	Luminosity	Total
L3	0.10	0.04	0.11
ALEPH	0.10	0.04	0.11
OPAL	0.08	0.03	0.09
DELPHI	0.13	0.04	0.14

5.4 Cross-talk scans

It is possible that a vernier adjustment at one IP may influence the mis-crossing of the beams at the other IP's. This is known as Vernier cross-talk and is predicted to be roughly -10% [15] [16]. In other words a Vernier induced shift at one IP will lead to a 10% shift in the opposite direction at each of the other IP's.

This was tested by observing the shift of the optimal Vernier position when a test IP (IP6) was forced to $+$ and $-$ 5 μm from the IP6 optimal Vernier setting. This shift of 10 μm is then expected to produce a $\sim 1 \mu m$ shift at each of the three other IP's. The result of this test is shown in figure 9. The magnitude and sign of the effect are reproduced [17].

The mean over all families is 15% and it is observed that the family shape is distorted in IP4 and IP8 as if there were no cross-talk for family c in those IP's.

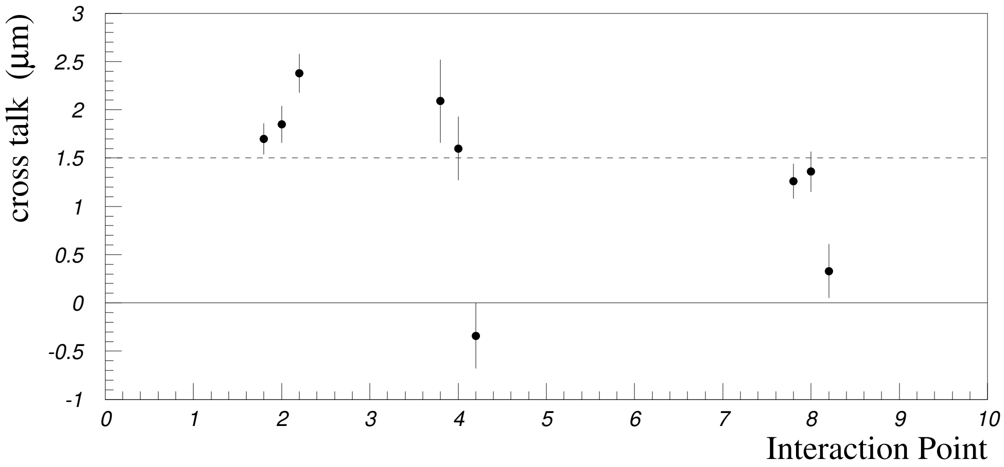

Figure 9: *The observed shift in the optimal Vernier setting at each IP due to a $10 \mu m$ shift at IP6. The three points at each IP are families a,b and c from left to right.*

Since a majority of Vernier scans were done in order around the LEP ring, it is possible that the trim which were done after each Vernier scan (to control the collision offsets) might add coherently and cause a systematic shift in collision offsets at the IP's which were trimmed earlier. The trim distributions were investigated and it was found that there could be *at most* a 0.1 MeV systematic error at IP2 and smaller errors at IP's 4,6 and 8 [14]. This effect assumes that the trims are fully correlated. Since the correlation is small, this effect is neglected.

The prediction [16] of the Vernier cross-talk also extends to the same IP. The -15% (measured) effect is expected to occur at *all* IP's. This effectively results in a change in the Vernier scale of 15%. We know that the overall scale doesn't effect the determination of ΔE_{cm} for reasons given in section 2.4.

The cross-talk does however have an effect on the measurement of the dispersion difference because of the measurement technique. The shift in RF frequency effectively shifts all IP so that their cross-talk acts on the IP of the dispersion measurement [18]. This effect is expected to change the dispersion difference measurements by ~ 0.1 mm. This error introduces a negligible error on ΔE_{cm}.

5.5 Correlation of optimal settings

Another indication that the optimal Vernier setting drifts are real is the observation that they are positively correlated between IP's. Figure 10 shows an example of this correlation. The same correlation is apparent for all IP's at both off peak energies.

Since the correlations are positive for all IP's and since the dispersion differences alternate in sign for each IP, the energy corrections will tend to cancel when all of the luminosities from the 4 IP's are added together.

The correlation coefficients are roughly 0.4 between IP's. Since this will tend to reduce the final statistical error from collision offsets (once the results from the different IP's are combined) we will conservatively ignore this effect.

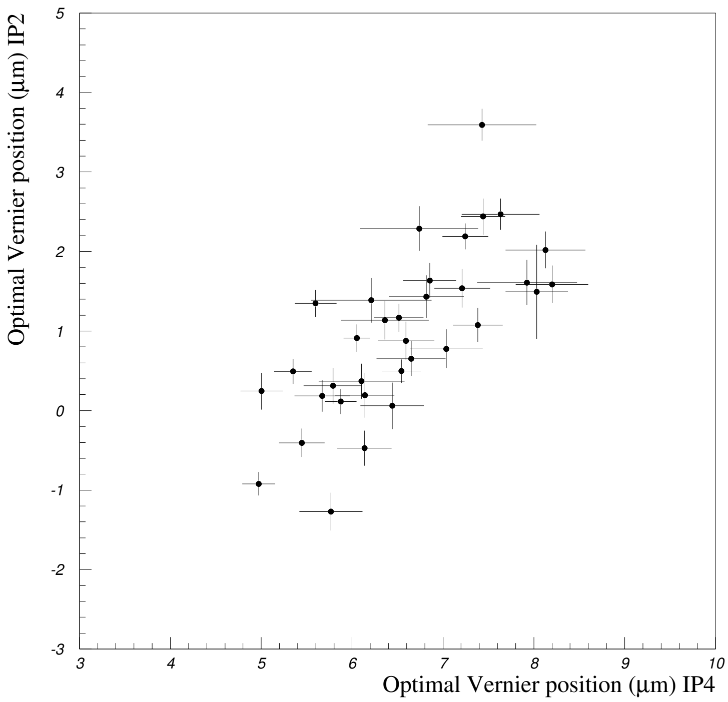

Figure 10: *The correlation between the optimal Vernier setting for IP2 and IP4 at peak−2.*

5.6 Systematic drift within a fill

Another possible effect associated with Vernier scans is bias in the sampling of the *true* optimal position. This can be thought of as similar to the resonant depolarization bias coming from the magnetic field rise and the fact that most depolarizations were done at the end of fill. The bias due to Vernier scans is much smaller since they were more evenly distributed throughout the fill. In fact, 35% of all of the integrated luminosity in the off peak points were taken prior to the first Vernier scan. 47% was taken between two Vernier scans and 17% was taken after the last Vernier scan. This asymmetry of 35 - 17 = 18% is taken as the possible luminosity bias.

We next consider systematic drifts in the y_{opt} from the Vernier scans. To do this we fit y_{opt} vs. the time into the fill in hours to a straight line [3)]. An example of this is shown in

Figure 11. If we take the extreme situation and assume that the entire 18% is taken at the intercept then we can get a conservative estimate of the systematic error associated with this behaviour. Table 11 shows the intercept at each IP and each off peak point. Also included is the energy shift assuming all 18% of the integrated luminosity is taken at the intercept. Note the similar behaviour at peak-2 and peak$+2$. We will take this as a systematic error and fully correlated between energies. For simplicity and since the error is small we will also take this error to be correlated among the different interaction points.

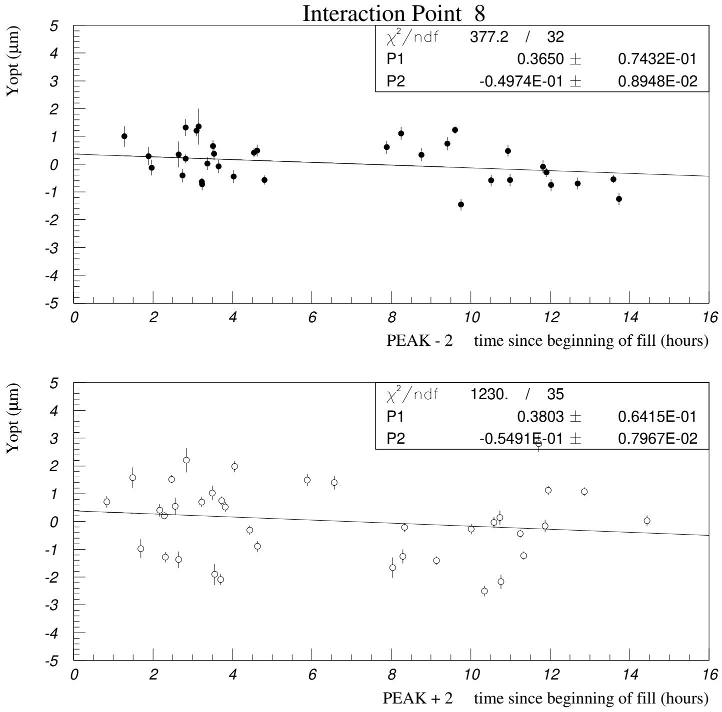

Figure 11: *The drift of the optimal Vernier setting as a function of time into the fill.*

5.7 Model and fit comparison

When we compare the results of the collision offsets when we use the simple gaussian fit or the beam size corrected fit we find a mean difference of 0.00 μm with an rms difference of 0.05 μm. This is when comparing the mean for the scan period at each IP at each energy point.

A comparison has been made with another model of collision offsets which uses the BEUV in the fit for the optimal position and has other minor differences in the implementation of the model [19]. This comparison finds a mean difference of -0.02 μm with an rms difference of 0.14 μm.

These are taken together as an uncorrelated systematic error of 0.15 μm for the determination of the collision offset.

---

[3] We have removed the drift over the 1995 energy scan period such that the average of the straight line fit is zero.

Table 11: *Intercept (μm) and energy shift (MeV) at each IP and off peak energy.*

Intercept and Energy shift		
IP	Intercept(μm)	ΔE_{cm}(MeV)
L3 Peak-2	0.09	-0.04
L3 Peak+2	0.21	-0.09
ALEPH Peak-2	-0.19	-0.05
ALEPH Peak+2	-0.21	-0.05
OPAL Peak-2	0.24	-0.06
OPAL Peak+2	0.36	-0.09
DELPHI Peak-2	0.37	0.11
DELPHI Peak+2	0.38	0.11

5.8 Vertical Beam Size

In addition to the 0.5 μm error on the vertical beam size, we also compare the results of the energy shifts using an average beam size given by equation 3 and energy shift where the model of the beam size is used as a function of time into the fill and for each energy. The rms variation of the difference is 0.13 MeV when comparing at all IP's and energy points. This will be added to the error coming from the 0.5 μm beam size error which typically produces and error of $\sim$ 0.1 MeV.

5.9 Combining all of the errors

Most of the errors are uncorrelated between the different IP's and energies. Table 12 lists these for each IP and energy. In the case of the ΔD_y^* and σ_y systematic error, the larger of the ΔE_{cm} shift or the statistical error (from table 8) is used.

Including the statistical errors (from table 8) with the uncorrelated systematic errors and combining all of the IP's together allows us to estimate the error on each energy point once all of the experiments are combined. This is given in table 13.

The correlated error is dominated by the reverse bias which was discussed in section 5.1. Also included is the larger of the drift errors given in table 11. These are shown in table 14.

An average (over the energy points) of the statistical, and systematic errors is given in table 15 for each experiment.

Table 12: *Uncorrelated systematic errors for ΔE_{cm} for each IP and energy.*

ΔE_{cm} uncorrelated systematic errors (MeV)					
IP	ΔD_y^*	σ_y	fit	fam-fam	Total
L3 Peak−2	0.20	0.30	0.35	0.11	0.51
L3 Peak	0.17	0.26	0.35	0.11	0.48
L3 Peak−2	0.08	0.17	0.35	0.11	0.41
ALEPH Peak−2	0.24	0.19	0.19	0.11	0.38
ALEPH Peak	0.14	0.15	0.19	0.11	0.30
ALEPH Peak−2	0.17	0.16	0.19	0.11	0.32
OPAL Peak−2	0.21	0.17	0.21	0.09	0.35
OPAL Peak	0.18	0.16	0.21	0.09	0.33
OPAL Peak−2	0.18	0.16	0.21	0.09	0.33
DELPHI Peak−2	0.14	0.15	0.24	0.14	0.35
DELPHI Peak	0.42	0.27	0.24	0.14	0.57
DELPHI Peak−2	0.18	0.16	0.24	0.14	0.37

Table 13: *The combined uncorrelated errors on ΔE_{cm} for each energy point.*

Uncorrelated error on ΔE_{cm}	
Energy	$\delta\Delta E_{cm}$ (MeV)
Peak − 2	0.24
Peak	0.31
Peak − 2	0.25

Table 14: *The correlated errors on ΔE_{cm}.*

ΔE_{cm} correlated systematic errors			
IP	Reverse	Drift	Total
L3	0.30	0.09	0.31
ALEPH	0.17	0.05	0.18
OPAL	0.18	0.09	0.20
DELPHI	0.21	0.11	0.24

Table 15: *Mean statistical and systematic errors on ΔE_{cm} for each IP. The systematic errors are labeled uncorrelated and correlated.*

Errors on ΔE_{cm} (MeV)			
IP	Statistical	Uncorrelated	Correlated
L3	0.39	0.46	0.31
ALEPH	0.24	0.35	0.18
OPAL	0.37	0.34	0.20
DELPHI	0.32	0.36	0.24

6 Conclusion

The effect of dispersion and collision offsets has been analyzed in the 1995 LEP energy scan of the Z^o. The program of performing Vernier scans during the fills and adjusting accordingly was successful in keeping the collision offsets low as well as providing the necessary information to evaluate the scale of the effect and systematic errors. Statistical and systematic errors have been evaluated for each IP and at each energy scan point. The expected error on the mass and width of the Z^o from this effect (once the results from all experiments are combined) is $\sim$ 0.3 MeV. The effect on an individual experiment is roughly twice that.

References

[1] J.M.Jowett, J.Wenninger, J.Yamartino, 'Influence of Dispersion and Collision offsets on the Centre-of-Mass Energy at LEP', CERN-SL/note 95-46(OP) (1995).

[2] E. Keil, 'Truly Self-Consistent Treatment of the Side Effects with Bunch Trains', CERN SL/95-75 (1995).

[3] The LEP Energy Working Group, 'LEP Center-of-Mass Energies in Presence of Opposite Sign Vertical Dispersion in Bunch-Train Operation', LEP Energy Group/95-2 (1995).

[4] J. Yamartino, contribution to the 76th LEP Energy WG meeting (Aug. 18 1995).

[5] P. Puzo, contribution to the 78th LEP Energy WG meeting (Sep. 21 1995).

[6] A. Blondel, contribution to the 68th LEP Energy WG meeting (May 29 1995).

[7] M. Lamont, private communication.

[8] A. Blondel, contribution to the 67th LEP Energy WG meeting (May 12 1995).

[9] The momentum compaction factor was remeasured in 1995 and found to be equal to previous measurements.

[10] P. Puzo, contribution to the 81st LEP Energy WG meeting (Oct. 26 1995).

[11] J. Yamartino, contribution to the 96th LEP Energy WG meeting (Jun. 21 1996).

[12] A. Blondel, E. Lançon, Detailed note in praparation.

[13] J. Yamartino, contribution to the 93th LEP Energy WG meeting (May 31 1996).

[14] J. Yamartino, contribution to the 95th LEP Energy WG meeting (Jun. 14 1996).

[15] E. Keil, contribution to the 70th LEP Energy WG meeting (Jul. 3 1995).

[16] F. C. Iselin, the `train` program.

[17] M. Hildreth, contribution to the 79th LEP Energy WG meeting (Sep. 29 1995).

[18] J. Yamartino, contribution to the 80th LEP Energy WG meeting (Oct. 13 1995).

[19] M. Koratzinos, contribution to the 78th LEP Energy WG meeting (Sep. 21 1995).